ACS APPLIED MATERIALS & INTERFACES

Research Article

www.acsami.org

Coordination-Mediated Programmable Assembly of Unmodified Oligonucleotides on Plasmonic Silver Nanoparticles

Dan Zhu,[†] Jie Chao,[‡] Hao Pei,[†] Xiaolei Zuo,*[,†] Qing Huang,[†] Lianhui Wang,[‡] Wei Huang,[‡] and Chunhai Fan*[,†]

[†]Division of Physical Biology & Bioimaging Center, Shanghai Synchrotron Radiation Facility, Shanghai Institute of Applied Physics, Chinese Academy of Sciences, Shanghai 201800, China

[‡]Key Laboratory for Organic Electronics & Information Displays (KLOEID) and Institute of Advanced Materials (IAM), Nanjing University of Posts & Telecommunications, Nanjing 210046, China

Supporting Information

ABSTRACT: DNA-decorated metal nanoparticles have found numerous applications, most of which rely on thiolated DNA (SH-DNA)-modified gold nanoparticles (AuNPs). Whereas silver nanoparticles (AgNPs) are known to have stronger plasmonic properties than AuNPs, modification of AgNPs with SH-DNA is technically challenging, partially due to the instability of Ag−S bonding. Here we demonstrate a facile approach to self-assemble unmodified DNA on AgNPs by exploiting intrinsic silver−cytosine (Ag−C) coordination. The strong Ag−C coordination allows for the ready formation of DNA-AgNP conjugates, which show favorable stability under conditions of high ionic strength and high temperature. These nanoconjugates possess much higher efficient molecular recognition capability and faster hybridization kinetics than thiolated DNA-modified AgNPs. More importantly, we could programmably tune the DNA density on AgNPs with the regulation of silver−cytosine coordination numbers, which in turn modulated their hybridizability. We further demonstrated that these DNA-AgNP conjugates could serve as excellent building blocks for assembling silver and hybrid silver−gold nanostructures with superior plasmonic properties.

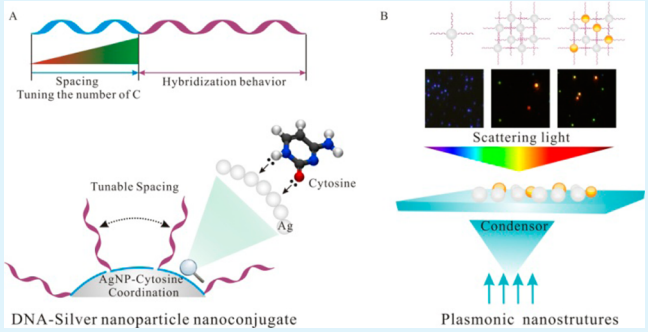

KEYWORDS: *coordination, silver nanoparticle, programmable assembly, umodified DNA, plasmonic*

INTRODUCTION

DNA-decorated nanoparticles have become popular tools in a variety of areas including bioelectronics, biosensors, bioimaging, and drug delivery.[1−14] A type of particularly useful nanoconjugates is gold nanoparticles (AuNPs) modified with thiolated DNA.[1−3,6,8,9,11,14] Other examples include DNA-modified silver nanoparticles[4] (AgNPs), quantum dots (QDs),[13,15] iron oxide nanoparticles,[16,17] and upconversion nanoparticles.[18] Among these, DNA-modified AgNPs are relatively poorly explored,[19] despite the fact that AgNPs possess many unique properties, such as high conductivity, strong plasmonic property, and excellent antibacterial ability.[7,20−23] The reason for this largely comes from the difficulty in making stable and functional conjugates of DNA-AgNPs using the conventional protocols with thiolated DNA, partially due to the easily oxidizable property of AgNPs.[19,24,25] Whereas there have been several methods to prepare DNA-AgNP conjugates with sophisticated protocols, e.g., the use of DNA with special modifications of disulfide, thioctic acid, or cyclic disulfide,[19,26] it remains a hurdle to facilely and controllably assemble DNA on AgNPs.[19] In this work, we report on a highly programmable strategy to synthesize DNA-AgNP conjugates by exploiting the specific silver−cytosine (Ag−C) coordination (Figure 1).

Metal−ligand coordination has been widely exploited to drive self-assembly in nature and in artificial systems,[27−35] e.g., supramolecules and nanoparticles. Recent progress in rational design with metal−ligand coordination has led to arrays of two-dimensional (2D; triangles, rectangles, and squares) and three-dimensional (3D; cubes, cages, and pyramids) systems.[29,36] In these supramolecular systems, both thermodynamic and kinetic properties can be readily controlled and finely regulated.[29,32] Other elegant examples include assembly of protein superstructures,[37] self-assembly of DNA-based metal arrays,[38,39] targeting, and crystallization of proteins.[40] It is especially interesting to note that several types of metal elements can specifically coordinate with DNA bases, which include mercury−thymine[41] (Hg−T) and silver−cytosine[42] (Ag−C). These unique coordination interactions have been exploited to develop new methods for nucleic acid detection, biosensing,

Received: April 8, 2015
Accepted: April 22, 2015
Published: April 22, 2015

DOI: 10.1021/acsami.5b03066
ACS Appl. Mater. Interfaces 2015, 7, 11047−11052

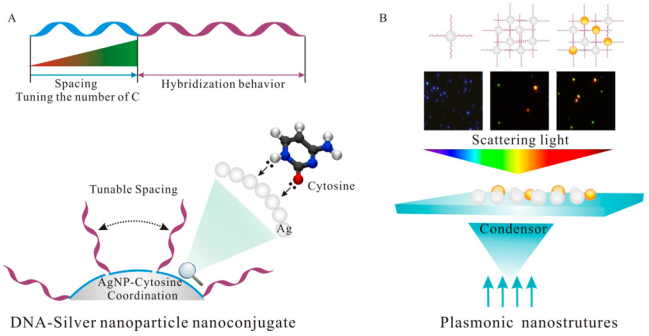

Figure 1. (A) Silver−cytosine coordination mediated self-assembly of DNA-AgNP nanoconjugates. The number of cytosines can be easily regulated. Hence, the DNA density, hybridization capability, and stability of nanoconjugates can be programmably regulated. (B) The DNA-AgNPs nanoconjugates can be assembled into plasmonic nanostructures (Ag−Ag nanostructures and Ag−Au hybrid nanostructures) with superior plasmonic property.

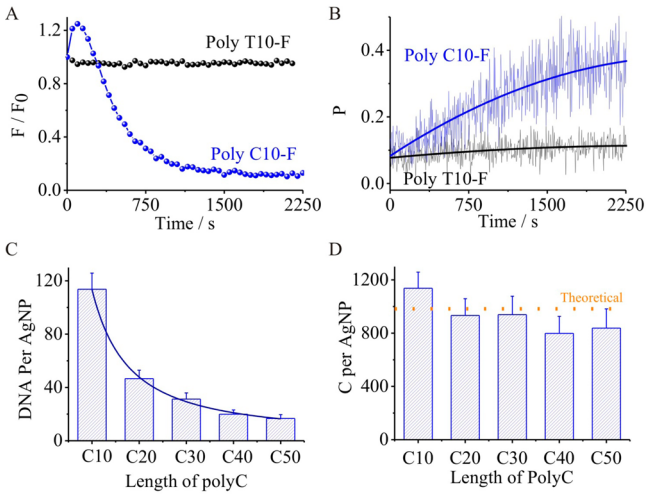

Figure 2. (A) Fluorescence quenching of polyC10-F and polyT10-F by mixing them with AgNPs in PBS of 10 mM at 298 K. (B) The increase of fluorescence polarization demonstrated that polyC10-F preferentially adsorbed onto AgNPs. No obvious change was observed for polyT10-F. (C) The surface density of DNA on AgNPs can be programmably regulated by tuning the number of cytosines (poly C10, poly C20, poly C30, poly C40, poly C50). (D) Normalized cytosine bases on AgNPs were almost identical and independent of the length of polyC.

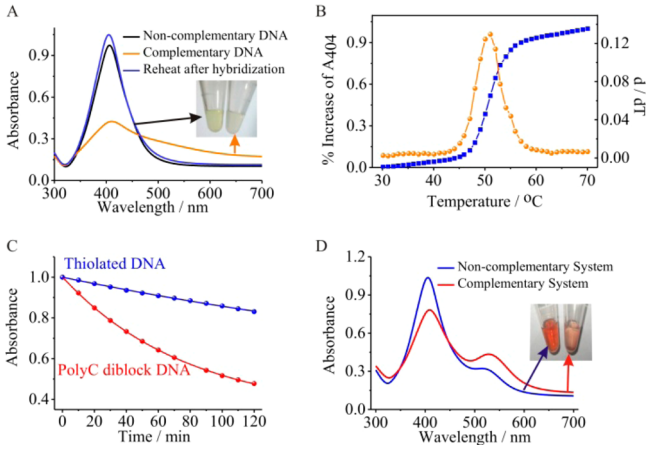

Figure 3. (A) UV−vis spectra and photographs of noncomplementary diblock DNA-AgNP conjugates (black line) and hybridized diblock DNA-AgNP conjugates (orange line). After heating, the hybridized complex converted to dispersed nanoconjugates (blue line). (B) Melting curves are shown of hybridized DNA−AgNP aggregates which were monitored by the extinction of the AgNPs at 404 nm as a function of temperature. The melting transition is extremely sharp. (C) The hybridization kinetics are plotted for the complementary diblock DNA−AgNPs (orange dots) and SH—DNA−AgNPs (blue dots). The line is the fitting by the second-order reaction. (D) UV−vis spectra and photographs are given of the mixture of AgNPs and AuNPs functionalized with complementary (orange line) and noncomplementary (blue line) diblock DNA.

and bioimaging, when coupled with the high sequence-specific recognition ability of nucleic acids. However, little attention has been paid to coordination of cytosine with silver atoms on the surface of AgNPs.

We reason that consecutive cytosines (polyC) should mediate the assembly of DNA oligonucleotides on AgNPs. This appears to resemble our previously reported polyA-mediated assembly strategy on AuNPs.[43] Nevertheless, the driving force in this system lies in the specific silver−cytosine coordination rather than nonspecific Au−polyA interactions. We also reason that the presence of multivalent Ag−C coordination should stabilize the nanoconjugates, a key problem that is often encountered in preparing DNA-AgNP nanoconjugates. As a step further, we programmably control the density of anchored DNA molecules, and examine the resulting hybridization ability. We also employ these DNA-AgNP conjugates as building blocks to assemble plasmonic nanostructures.

RESULTS AND DISCUSSION

We first examined the coordination ability of cytosine on the surface of AgNPs. To interrogate their coordination, we employed a fluorophore (FAM; carboxyfluorescein) labeled oligonucleotide with 10 consecutive cytosines (polyC10-F) to study its interactions with AgNPs. When polyC10-F was mixed with AgNPs, we observed a slight increase in the fluorescence intensity, followed by a drastic decrease of the emission (Figure 2A). The slight increase may originate from the metal surface enhanced fluorescence of FAM when the FAM is localized near the surface of AgNPs because of the binding of cytosine with AgNP. Then the multiple Ag−C coordination forced the FAM further close to the metal core, leading to significant silver-induced fluorescence quenching of FAM.[44] In a relatively short time scale (within 20 min), the fluorescence was almost totally quenched. These results indicated that the polyC10-F was adsorbed on the surface of AgNPs.

We further testified to the specificity of the Ag−C coordination by replacing the cytosine with thymine. A control study with FAM-labeled DNA of 10 consecutive thymines (polyT10-F) showed minimal variation of the fluorescence intensity in 20 min, suggesting the absence of binding between polyT10-F and AgNPs (Figure 2A). Fluorescence polarization studies further confirmed the preferential binding between polyC10-F and AgNPs (Figure 2B). We found that the fluorescence polarization from the polyC10-F increased substantially upon being mixed with AgNPs, suggesting the decrease of the rotation and tumbling of FAM due to the occurrence of binding, whereas polyT10-F and AgNPs showed negligible change in fluorescence polarization, which indicated no binding occurred.

DOI: 10.1021/acsami.5b03066
ACS Appl. Mater. Interfaces 2015, 7, 11047−11052

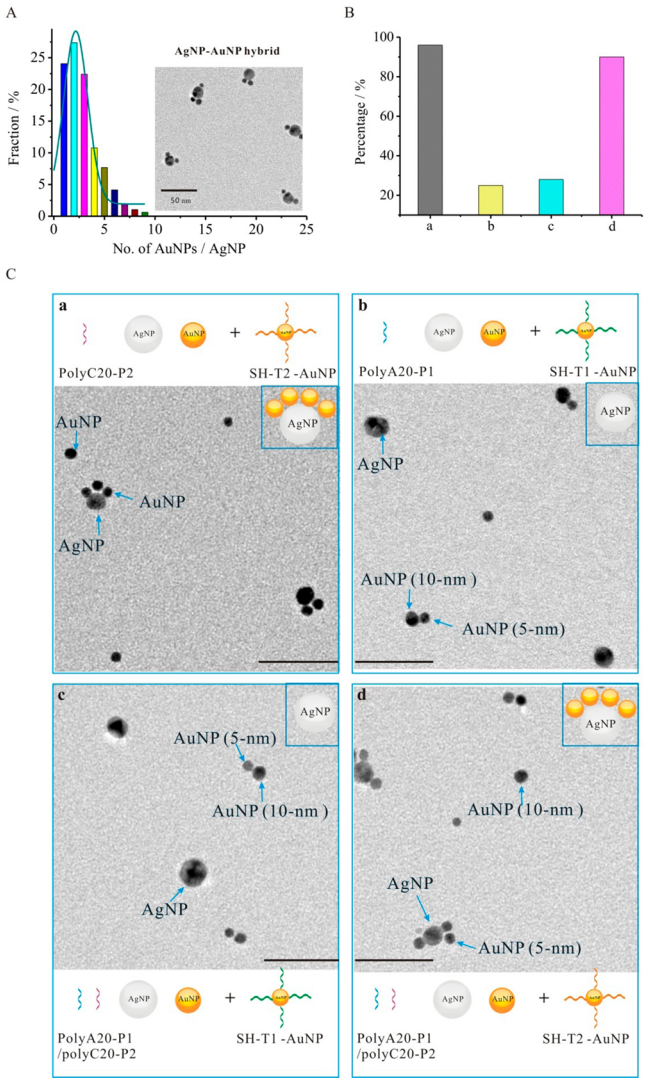

Figure 4. (A) TEM image of hybrid AgNP-AuNP nanoconjugates and statistical analysis of the AuNPs distributions on AgNP. (B) Statistical analysis is shown of the percentage of AgNPs conjugated with AuNPs in our competition experiments. (C(a)) 20 nm of AgNPs and 10 nm of AuNPs were mixed with polyC20-P2. SH-T2-AuNPs (5 nm) were then added for hybridization. The TEM image demonstrated that most of the AgNPs were conjugated with AuNPs (5 nm). (C(b)) 20 nm of AgNPs and 10 nm of AuNPs were mixed with polyA20-P1. SH-T1-AuNPs (5 nm) were then added for hybridization. All of the AgNPs were kept unconjugated. (C(c)) TEM image demonstrated AgNPs were not conjugated with SH-T1-AuNPs (5 nm), which indicated that polyA20-P1 was not adsorbed on AgNPs. (C(d)) AgNPs were conjugated with SH-T2-AuNPs (5 nm) indicating that polyC20-P2 was preferentially adsorbed on AgNPs. Scale bar: 50 nm.

We assembled DNA on AgNPs by using polyC as an anchoring block and investigated the stability of DNA-AgNP nanoconjugates. By the employment of Ag−C coordination, we designed a diblock DNA (polyC20-P1) containing 20 consecutive cytosines (polyC20) and a single-stranded DNA region (P1) for the self-assembly of DNA-AgNP nanoconjugates. The absorbance spectrum of polyC20-P1-AgNP conjugates was nearly identical to that of well-dispersed unmodified AgNPs, indicating the formation of well-dispersed DNA-AgNP nanoconjugates. The nanoconjugates demonstrated high stability (Supporting Information (SI) Figure S1), even at high concentration of salt (300 mM of NaCl) or high temperature (up to 90 °C) (SI Figure S1), while AgNPs conjugated with DNA without polyC anchoring block aggregated immediately in a solution containing 300 mM NaCl.

We programmably regulated the length of the consecutive cytosines (polyC), which, in turn, can control the DNA density on the surface of AgNPs. We employed diblock DNA with different lengths of polyC to prepare DNA-AgNP nanoconjugates (Figure 2C). We quantified the density of diblock DNA on AgNPs according to the fluorescence-based method developed by Graham et al.[26] We achieved a series of nanoconjugates with well-controlled DNA densities. The DNA density was monotonically decreased with the increasing length of polyC in diblock DNA (Figure 2C). When we normalized the DNA density to the density of cytosine bases, we found that the cytosine density of each system was constant at 800−1000 per particle (Figure 2D), which was consistent with the theoretical cytosine density of a fully covered AgNP with cytosine bases (if the surface of AgNP (20 nm) was fully covered by cytosine bases, the amount of cytosine bases should be ∼980 per particle). This result indicated that the AgNP was fully covered by cytosine bases, which would be a benefit to prevent the nonspecific adsorption of other bases in the diblock DNA because no free sites on the AgNPs would be left.

We further investigated the stability of DNA-AgNP nanoconjugates with different lengths of polyC. We observed that the stability of these nanoconjugates (which were investigated by the treatment of DTT (1 mM) according to the well-developed method[26] (SI Figures S2 and S3 and Table S1)) was regulated by tuning the length of polyC. When the number of silver−cytosine coordination sites increased from 10 to 50, the half-life gradually increased from ∼13 to ∼33 min and the shift of λ_{max} in 60 min decreased from ∼58 to ∼52 nm, which indicated great enhancement in stability.

Having established the successful assembly of diblock DNA on AgNPs, we started to examine the hybridization ability of the recognition block on AgNPs. We employed two types of diblock DNA (polyC20-P1 and polyC20-T1; the recognition part P1 of polyC20-P1 is complementary to the counterpart T1 of polyC20-T1) to prepare DNA-AgNP conjugates, respectively. To demonstrate the hybridization ability of these two types of nanoconjugates, we investigated the hybridization of equal molar polyC20-P1-AgNP conjugates and polyC20-T1-AgNP conjugates (Figure 3A). Interestingly, we observed an obvious color change from bright yellow to light gray, which indicated the successful aggregation of these two types of nanoconjugates introduced by hybridization (Figure 3A). The plasmonic peak at 404 nm decreased dramatically, whereas another plasmonic peak at ∼550 nm increased. Interestingly, the aggregation introduced by the hybridization behavior was fully reversible. To prove this, we heated the solution and the color of the solution returned to bright yellow. At the same time, the plasmonic peak at 404 nm recovered, which indicated the dehybridization of the nanoconjugates. The hybridization and melting behaviors of DNA-modified AgNPs were fully retained. As a control experiment, we mixed two types of nanoconjugates with noncomplementary DNA and observed no change both in color and plasmonic peaks (Figure 3A). We further measured the melting curve of the hybridized nanoconjugates. An extremely sharp melting transition at ∼50 °C was observed (Figure 3B), which further indicated the aggregation and dispersion of AgNPs were induced by DNA hybridization.

DOI: 10.1021/acsami.5b03066
ACS Appl. Mater. Interfaces 2015, 7, 11047−11052

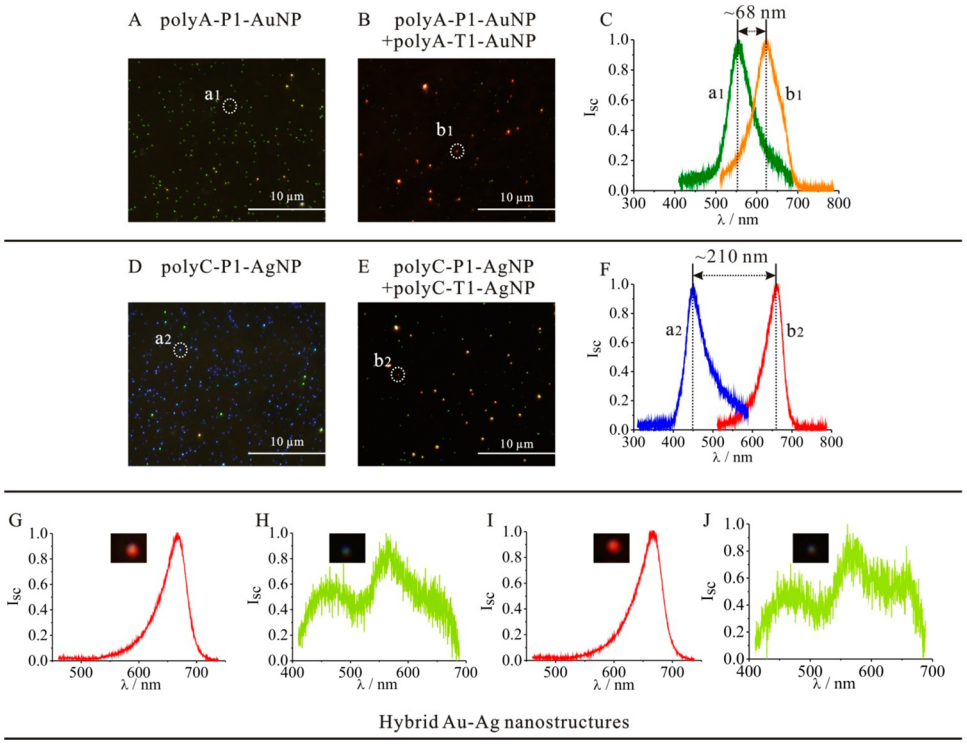

Figure 5. Dark field microscopy (DFM) images for polyA-P1-AuNP nanoconjugates (A), hybridized aggregates of polyA-P1-AuNP and polyA-T1-AuNP conjugates (B), polyC-P1-AgNP nanoconjugates (D), and hybridized aggregates of polyC-P1-AgNP and polyC-T1-AgNP nanoconjugates (E). (C and F) The light scattering spectra correspond to individual nanostructures marked with the circles in the DFM images. (Bottom panels) Dark field images and corresponding light scattering spectra shown of the hybridization of polyC-P1-AgNP conjugates and polyA-T1-AuNP conjugates at different polarization angles (0° (G), 90° (H), 180° (I), and 270° (J)).

We further investigated the hybridization kinetics of the DNA-AgNP nanoconjugates. The hybridization processes of DNA-AgNP nanoconjugates were monitored by continuously recording the plasmonic peak at 404 nm for 2 h (SI Figure S4). As a contrast, we also detected the hybridization kinetics of SH-DNA-AgNP conjugates (SI Figure S4). Surprisingly, the silver−cytosine coordination mediated nanoconjugates (Figure 3C) exhibited obvious faster hybridization kinetics than that of SH-DNA-AgNP nanoconjugates. The hybridization curves of these two systems were fitted using a second-order rate equation. The rate constant was 4.5 times faster than that of SH-DNA-AgNP conjugates. The fast kinetics probably originated from the favorable configuration of DNA on the surface of AgNPs, which was similar to our previously reported polyA-AuNP nanoconjugates.[43]

More interestingly, we attempted to construct AuNP-AgNP hybrid nanoconjugates by employing the polyC20-P1-AgNP conjugates and the DNA-AuNP conjugates. We observed an obvious color change from orange-red to pale red (Figure 3D). The plasmonic peaks shifted from 404 to 407 nm and from 514 to 528 nm, respectively, suggesting the aggregation of AuNPs and AgNPs upon DNA hybridization.

Next, we characterized the assembled hybrid AgNP (20 nm)-AuNP (5 nm) nanoconjugates by transmission electron microscopy (TEM) and statistically analyzed the distribution of AgNPs on AuNP (~2 AuNPs on a AgNP in average (Figure 4A). Then, we designed a set of competition experiments to examine the specificity of Ag−C coordination. We first mixed AgNPs of 20 nm and AuNPs of 10 nm in a solution. A diblock DNA (polyC20-P2) with 20 consecutive cytosines and a recognition segment P2 was then added to the mixture. To visualize the competition results with TEM, we further added 5 nm AuNPs conjugated with thiolated DNA (SH-T2) that was complementary to the recognition segment of polyC20-P2. Interestingly, we found that nearly all AgNPs (~96%, data were collected from 150 AgNPs) were assembled with 5 nm AuNPs whereas 10 nm AuNPs were left free (Figure 4B,C(a)). Hence, we established that polyC could preferentially bind to AgNPs via the Ag−C coordination, whereas polyC could not bind to AuNPs. As a control experiment, we added polyA20-P1 (a diblock DNA with 20 consecutive adenines and a recognition segment P1) to the mixture of AgNPs of 20 nm and AuNPs of 10 nm; then we added the 5 nm AuNPs conjugated with SH-T1 (complementary sequence of P1). Since the polyA sequences can preferentially bind to AuNPs as in our previous reports,[43] we observed that no AgNP was assembled with 5 nm AuNPs, indicating no preferential binding of polyA sequence and AgNPs (Figure 4C(b)).

To further substantiate such specificity, we added both polyC20-P2 and polyA20-P1 to the mixture of AgNPs and AuNPs, which were followed by the addition of 5 nm AuNPs modified with either SH-T2 or SH-T1. AuNPs functionalized with SH-T2 can be conjugated on silver nanoparticles (up to 90% (Figure 4B); data were collected from 641 AgNPs), whereas AuNPs functionalized with SH-T1 cannot be conjugated on AgNPs, which verified the specificity of silver−cytosine coordination (Figure 4C(c,d)).

The diblock DNA-AgNP nanoconjugates demonstrated excellent plasmonic property. We first employed diblock DNA-AuNP nanoconjugates as contrast (50 nm in diameter for AuNPs). The DNA-AuNP nanoconjugates exhibited green scattering light with scattering peak at ~555 nm (Figure 5A).

DOI: 10.1021/acsami.5b03066
ACS Appl. Mater. Interfaces 2015, 7, 11047−11052

After hybridization with complementary DNA-AuNP nanoconjugates, the scattering peak shifted ~68 nm to longer wavelength (Figure 5 B,C). As a sharp contrast, the scattering peak of DNA-AgNP (40 nm in diameter for AgNPs) nanoconjugates upon hybridization shifted ~210 nm, which is 3 times larger than that of DNA-AuNP nanoconjugates (Figure 5 D−F). Interestingly, the hybrid nanoaggregates of the DNA-Ag nanoconjugates and the DNA-Au nanoconjugates bridged by DNA sequences presented anisotropic property, which led to the change of scattered color by changing polarization angles (Figure 5G−J).

CONCLUSIONS

The strong dependence of plasmonic property on the assembly of AgNPs makes it a challenging problem to control the assembly of AgNPs, which could in turn regulate the collective plasmonic properties. When the thiol-based method is used to assemble DNA on AgNPs, the resulting thiolated DNA-AgNP nanoconjugates exhibited limited stability and poor bioactivity,[19] which hampered the applications of AgNPs in plasmonics. Here, we have demonstrated a silver−cytosine coordination-mediated self-assembly of DNA-AgNP conjugates with fully retained hybridization behavior of DNA, faster hybridization kinetics, controlled DNA density, and enhanced stability. The DNA-Ag nanoconjugates exhibit excellent plasmonic property with larger plasmonic peak shift (3 times larger than that of DNA-AuNP nanoconjugates). The Au−Ag hybrid nanostructures exhibit interesting anisotropic plasmonic scattering.

Several other advantages of our strategy include the following: intrinsic Ag−C coordination serves as the driving force, which eliminates the complicated modification of DNA. The Ag−C coordination sites can be easily regulated by tuning the number of coordination cytosines, and through this, the DNA density can be easily controlled. Also, the stability of nanoconjugates can be greatly enhanced by increasing the coordination sites. Moreover, the DNA hybridization rate was evidently faster than that of SH-DNA-AgNPs, which can be applied to construct a fast biosensor platform. Therefore, this facile and cost-effective approach to assemble DNA-AgNP conjugates with controllable DNA density, favorable hybridization capability, and superior plasmonic property has potential applications in plasmonics, DNA nanotechnology, and biosensors.

ASSOCIATED CONTENT

Supporting Information

Full experimental procedures and supporting figures and tables (Figures S1−S4 and Tables S1 and S2). The Supporting Information is available free of charge on the ACS Publications website at DOI: 10.1021/acsami.5b03066.

AUTHOR INFORMATION

Corresponding Authors

*(X.Z.) E-mail: zuoxiaolei@sinap.ac.cn.
*(C.F.) E-mail:fchh@sinap.ac.cn.

Notes

The authors declare no competing financial interest.

ACKNOWLEDGMENTS

This work was supported by the National Basic Research Program (973 Program 2012CB932600), the 100-talent project from the Chinese Academy of Sciences, the Shanghai Pujiang Project with Grant No. 13PJ1410700, and National Natural Science Foundation of China (NSFC, 21422508, 31470960).

REFERENCES

(1) Anker, J. N.; Hall, W. P.; Lyandres, O.; Shah, N. C.; Zhao, J.; Van Duyne, R. P. Biosensing with Plasmonic Nanosensors. *Nat. Mater.* **2008**, *7*, 442−453.
(2) Auyeung, E.; Cutler, J. I.; Macfarlane, R. J.; Jones, M. R.; Wu, J. S.; Liu, G.; Zhang, K.; Osberg, K. D.; Mirkin, C. A. Synthetically Programmable Nanoparticle Superlattices using a Hollow Three-Dimensional Spacer Approach. *Nat. Nanotechnol.* **2012**, *7*, 24−28.
(3) Elbaz, J.; Cecconello, A.; Fan, Z. Y.; Govorov, A. O.; Willner, I. Powering the programmed nanostructure and function of gold nanoparticles with catenated DNA machines. *Nat. Commun.* **2013**, *4*, No. 2000.
(4) Graham, D.; Thompson, D. G.; Smith, W. E.; Faulds, K. Control of Enhanced Raman Scattering using a DNA-Based Assembly Process of Dye-Coded Nanoparticles. *Nat. Nanotechnol.* **2008**, *3*, 548−551.
(5) Hura, G. L.; Tsai, C. L.; Claridge, S. A.; Mendillo, M. L.; Smith, J. M.; Williams, G. J.; Mastroianni, A. J.; Alivisatos, A. P.; Putnam, C. D.; Kolodner, R. D.; Tainer, J. A. DNA Conformations in Mismatch Repair Probed in Solution by X-ray Scattering from Gold Nanocrystals. *Proc. Natl. Acad. Sci. U. S. A.* **2013**, *110*, 17308−17313.
(6) Im, H.; Shao, H. L.; Park, Y. I.; Peterson, V. M.; Castro, C. M.; Weissleder, R.; Lee, H. Label-free Detection and Molecular Profiling of Exosomes with a Nano-plasmonic Sensor. *Nat. Biotechnol.* **2014**, *32*, 490−495.
(7) Kumar, A.; Vemula, P. K.; Ajayan, P. M.; John, G. Silver-Nanoparticle-Embedded Antimicrobial Paints Based on Vegetable Oil. *Nat. Mater.* **2008**, *7*, 236−241.
(8) Kuzyk, A.; Schreiber, R.; Zhang, H.; Govorov, A. O.; Liedl, T.; Liu, N. Reconfigurable 3D plasmonic metamolecules. *Nat. Mater.* **2014**, *13*, 862−866.
(9) (a) Liu, J. W.; Cao, Z. H.; Lu, Y. Functional Nucleic Acid Sensors. *Chem. Rev.* **2009**, *109*, 1948−1998. (b) Zhang, X.; Servos, M. R.; Liu, J. W. Fast pH-Assisted Functionalization of Silver Nanoparticles with Monothiolated DNA. *Chem. Commun. (Cambridge, U. K.)* **2012**, *48*, 10114−10116.
(10) Liu, N.; Tang, M. L.; Hentschel, M.; Giessen, H.; Alivisatos, A. P. Nanoantenna-Enhanced Gas Sensing in a Single Tailored Nanofocus. *Nat. Mater.* **2011**, *10*, 631−636.
(11) Macfarlane, R. J.; Lee, B.; Jones, M. R.; Harris, N.; Schatz, G. C.; Mirkin, C. A. Nanoparticle Superlattice Engineering with DNA. *Science* **2011**, *334*, 204−208.
(12) Schreiber, R.; Do, J.; Roller, E. M.; Zhang, T.; Schuller, V. J.; Nickels, P. C.; Feldmann, J.; Liedl, T. Hierarchical Assembly of Metal Nanoparticles, Quantum Dots and Organic Dyes using DNA Origami Scaffolds. *Nat. Nanotechnol.* **2014**, *9*, 74−78.
(13) Tikhomirov, G.; Hoogland, S.; Lee, P. E.; Fischer, A.; Sargent, E. H.; Kelley, S. O. DNA-Based Programming of Quantum Dot Valency, Self-Assembly and Luminescence. *Nat. Nanotechnol.* **2011**, *6*, 485−490.
(14) Zhang, C.; Macfarlane, R. J.; Young, K. L.; Choi, C. H. J.; Hao, L. L.; Auyeung, E.; Liu, G. L.; Zhou, X. Z.; Mirkin, C. A. A General Approach to DNA-Programmable Atom Equivalents. *Nat. Mater.* **2013**, *12*, 741−746.
(15) Deng, Z. T.; Samanta, A.; Nangreave, J.; Yan, H.; Liu, Y. Robust DNA-Functionalized Core/Shell Quantum Dots with Fluorescent Emission Spanning from UV-Vis to Near-IR and Compatible with DNA-Directed Self-Assembly. *J. Am. Chem. Soc.* **2012**, *134*, 17424−17427.
(16) Cutler, J. I.; Zheng, D.; Xu, X. Y.; Giljohann, D. A.; Mirkin, C. A. Polyvalent Oligonucleotide Iron Oxide Nanoparticle "Click" Conjugates. *Nano Lett.* **2010**, *10*, 1477−1480.
(17) Jiang, S.; Eltoukhy, A. A.; Love, K. T.; Langer, R.; Anderson, D. G. Lipidoid-Coated Iron Oxide Nanoparticles for Efficient DNA and SiRNA Delivery. *Nano Lett.* **2013**, *13*, 1059−1064.
(18) Li, L. L.; Zhang, R.; Yin, L.; Zheng, K.; Qin, W.; Selvin, P. R.; Lu, Y. Biomimetic Surface Engineering of Lanthanide-Doped

DOI: 10.1021/acsami.5b03066
ACS Appl. Mater. Interfaces 2015, 7, 11047−11052

Upconversion Nanoparticles as Versatile Bioprobes. *Angew. Chem.* **2012**, *51*, 6121−6125.
(19) Lee, J. S.; Lytton-Jean, A. K. R.; Hurst, S. J.; Mirkin, C. A. Silver Nanoparticle-Oligonucleotide Conjugates Based on DNA with Triple Cyclic Disulfide Moieties. *Nano Lett.* **2007**, *7*, 2112−2115.
(20) Christopher, P.; Xin, H. L.; Linic, S. Visible-Light-Enhanced Catalytic Oxidation Reactions on Plasmonic Silver Nanostructures. *Nat. Chem.* **2011**, *3*, 467−472.
(21) Lv, M.; Su, S.; He, Y.; Huang, Q.; Hu, W. B.; Li, D.; Fan, C. H.; Lee, S. T. Long-Term Antimicrobial Effect of Silicon Nanowires Decorated with Silver Nanoparticles. *Adv. Mater.* **2010**, *22*, 5463−5467.
(22) Rycenga, M.; Cobley, C. M.; Zeng, J.; Li, W. Y.; Moran, C. H.; Zhang, Q.; Qin, D.; Xia, Y. N. Controlling the Synthesis and Assembly of Silver Nanostructures for Plasmonic Applications. *Chem. Rev.* **2011**, *111*, 3669−3712.
(23) Tao, A.; Sinsermsuksakul, P.; Yang, P. Tunable plasmonic lattices of silver nanocrystals. *Nat. Nanotechnol.* **2007**, *2*, 435−440.
(24) Cao, Y. W.; Jin, R.; Mirkin, C. A. DNA-modified core-shell Ag/Au nanoparticles. *J. Am. Chem. Soc.* **2001**, *123*, 7961−7962.
(25) Tokareva, I.; Hutter, E. Hybridization of Oligonucleotide-Modified Silver and Gold Nanoparticles in Aqueous Dispersions and on Gold Films. *J. Am. Chem. Soc.* **2004**, *126*, 15784−15789.
(26) Dougan, J. A.; Karlsson, C.; Smith, W. E.; Graham, D. Enhanced Oligonucleotide-Nanoparticle Conjugate Stability using Thioctic Acid Modified Oligonucleotides. *Nucleic Acids Res.* **2007**, *35*, 3668−3675.
(27) Chakrabarty, R.; Mukherjee, P. S.; Stang, P. J. Supramolecular Coordination: Self-Assembly of Finite Two- and Three-Dimensional Ensembles. *Chem. Rev.* **2011**, *111*, 6810−6918.
(28) Liu, Y.; Yan, H. Coordinating Corners. *Nat. Chem.* **2009**, *1*, 339−340.
(29) Northrop, B. H.; Zheng, Y. R.; Chi, K. W.; Stang, P. J. Self-Organization in Coordination-Driven Self-Assembly. *Acc. Chem. Res.* **2009**, *42*, 1554−1563.
(30) Park, H. S.; Nam, S. H.; Lee, J. K.; Yoon, C. N.; Mannervik, B.; Benkovic, S. J.; Kim, H. S. Design and Evolution of New Catalytic Activity with an Existing Protein Scaffold. *Science* **2006**, *311*, 535−538.
(31) Wang, Y. F.; Hollingsworth, A. D.; Yang, S. K.; Patel, S.; Pine, D. J.; Weck, M. Patchy Particle Self-Assembly via Metal Coordination. *J. Am. Chem. Soc.* **2013**, *135*, 14064−14067.
(32) Yan, X. Z.; Li, S. J.; Pollock, J. B.; Cook, T. R.; Chen, J. Z.; Zhang, Y. Y.; Ji, X. F.; Yu, Y. H.; Huang, F. H.; Stang, P. J. Supramolecular Polymers with Tunable Topologies via Hierarchical Coordination-Driven Self-Assembly and Hydrogen Bonding Interfaces. *Proc. Natl. Acad. Sci. U. S. A.* **2013**, *110*, 15585−15590.
(33) Yang, H.; McLaughlin, C. K.; Aldaye, F. A.; Hamblin, G. D.; Rys, A. Z.; Rouiller, I.; Sleiman, H. F. Metal-Nucleic Acid Cages. *Nat. Chem.* **2009**, *1*, 390−396.
(34) Zhou, L.; Bosscher, M.; Zhang, C. S.; Ozcubukcu, S.; Zhang, L.; Zhang, W.; Li, C. J.; Liu, J. Z.; Jensen, M. P.; Lai, L. H.; He, C. A Protein Engineered to Bind Uranyl Selectively and with Femtomolar Affinity. *Nat. Chem.* **2014**, *6*, 236−241.
(35) Zhou, X. P.; Liu, J.; Zhan, S. Z.; Yang, J. R.; Li, D.; Ng, K. M.; Sun, R. W. Y.; Che, C. M. A High-Symmetry Coordination Cage from 38- or 62-Component Self-Assembly. *J. Am. Chem. Soc.* **2012**, *134*, 8042−8045.
(36) Stang, P. J. Abiological Self-Assembly via Coordination: Formation of 2D Metallacycles and 3D Metallacages with Well-Defined Shapes and Sizes and Their Chemistry. *J. Am. Chem. Soc.* **2012**, *134*, 11829−11830.
(37) Salgado, E. N.; Faraone-Mennella, J.; Tezcan, F. A. Controlling Protein−Protein Interactions through Metal Coordination: Assembly of a 16-Helix Bundle Protein. *J. Am. Chem. Soc.* **2007**, *129*, 13374−13375.
(38) Tanaka, K.; Clever, G. H.; Takezawa, Y.; Yamada, Y.; Kaul, C.; Shionoya, M.; Carell, T. Programmable Self-Assembly of Metal Ions Inside Artificial DNA Duplexes. *Nat. Nanotechnol.* **2006**, *1*, 190−194.
(39) Tanaka, K.; Tengeiji, A.; Kato, T.; Toyama, N.; Shionoya, M. A Discrete Self-Assembled Metal Array in Artificial DNA. *Science* **2003**, *299*, 1212−1213.
(40) Frey, W.; Schief, W. R.; Pack, D. W.; Chen, C. T.; Chilkoti, A.; Stayton, P.; Vogel, V.; Arnold, F. H. Two-Dimensional Protein Crystallization via Metal-Ion Coordination by Naturally Occurring Surface Histidines. *Proc. Natl. Acad. Sci. U. S. A.* **1996**, *93*, 4937−4941.
(41) Lee, J. S.; Han, M. S.; Mirkin, C. A. Colorimetric detection of mercuric ion (Hg^{2+}) in aqueous media using DNA-functionalized gold nanoparticles. *Angew. Chem., Int. Ed.* **2007**, *46*, 4093−4096.
(42) Wang, Y.; Luan, B. Q.; Yang, Z.; Zhang, X.; Ritzo, B.; Gates, K.; Gu, L. Q. Single Molecule Investigation of Ag(+) Interactions with Single Cytosine-, Methylcytosine- and Hydroxymethylcytosine-Cytosine Mismatches in a Nanopore. *Sci. Rep.* **2014**, *4*, No. 5883.
(43) Pei, H.; Li, F.; Wan, Y.; Wei, M.; Liu, H. J.; Su, Y.; Chen, N.; Huang, Q.; Fan, C. H. Designed Diblock Oligonucleotide for the Synthesis of Spatially Isolated and Highly Hybridizable Functionalization of DNA-Gold Nanoparticle Nanoconjugates. *J. Am. Chem. Soc.* **2012**, *134*, 11876−11879.
(44) Zhang, J.; Fu, Y.; Chowdhury, M. H.; Lakowicz, J. R. Metal-Enhanced Single-Molecule Fluorescence on Silver Particle Monomer and Dimer: Coupling Effect between Metal Particles. *Nano Lett.* **2007**, *7*, 2101−2107.

DOI: 10.1021/acsami.5b03066
ACS Appl. Mater. Interfaces 2015, 7, 11047−11052